International Journal of Humanoid Robotics
© World Scientific Publishing Company

THE DESIGN OF THE ICUB HUMANOID ROBOT

ALBERTO PARMIGGIANI[*], MARCO MAGGIALI[*], LORENZO NATALE[*], FRANCESCO NORI[*], ALEXANDER SCHMITZ[*], NIKOS TSAGARAKIS[†], JOSÉ SANTOS VICTOR[‖], FRANCESCO BECCHI[‡], GIULIO SANDINI[*§], GIORGIO METTA[*§]

[*]*Robotics Brain and Cognitive Sciences Department,*
Istituto Italiano di Tecnologia
Via Morego 30, 16163 Genova, Italy
alberto.parmiggiani@iit.it, marco.maggiali@iit.it, lorenzo.natale@iit.it, francesco.nori@iit.it, alexander.schmitz@iit.it, giulio.sandini@iit.it, giorgio.metta@iit.it

[†]*Advanced Robotics Department,*
Istituto Italiano di Tecnologia
Via Morego 30, 16163 Genova, Italy
nikos.tsagarkis@iit.it

[‖]*Institute of Systems and Robotics,*
Instituto Superior Técnico,
Av. Rovisco Pais, 1049-001 Lisboa, Portugal
jasv@isr.ist.utl.pt

[‡]*Telerobot OCEM s.r.l.,*
Via Semini 28C 16163 Genova, Italy
becchi@telerobot.it

[§]*DIST, University of Genoa,*
Viale Causa, 13 16145 Genova, Italy

Received 2^{nd} August 2010
Revised 1^{st} July 2011
Accepted Day Month Year

This article describes the hardware design of the iCub humanoid robot. The iCub is an open-source humanoid robotic platform designed explicitly to support research in embodied cognition. This paper covers the mechanical and electronic design of the first release of the robot. A series upgrades developed for the second version of the robot (iCub2), which are aimed at the improvement of the mechanical and sensing performance, are also described.

Keywords: humanoid robotics; open source; cognitive system.

1. Introduction

In recent years there has been a growing worldwide attention to the development of humanoid robots. Although these robots are intended for real world applications

most of them are at the moment at the status of research prototypes to address the problems of mobility[1,2], entertainment[3,4,5] and service robotics[6,7,8] to cite a few. Humanoid robots are also often used as a model to study human behaviour[9,10,11,12]. The iCub (shown in Fig.1) can be considered as a member of the latter category.

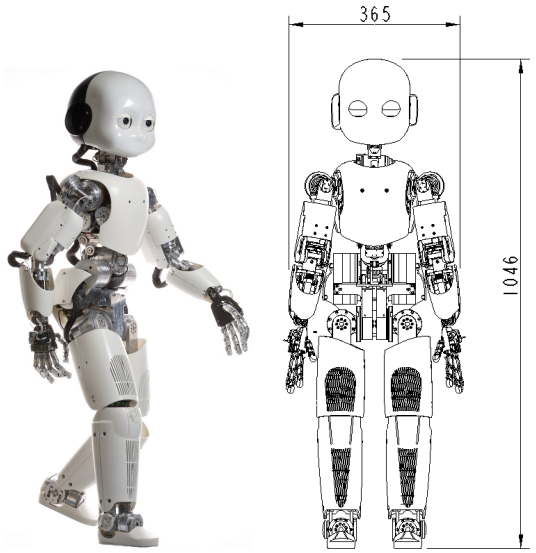

(a) (b)

Fig. 1. The iCub. The figure shows a photograph of the iCub robot (a). The overall robot dimensions are shown in (b).

2. RobotCub: open source robotics

Open source robotics, especially in its recent evolution, can be given two different flavors covering respectively the software components required to operate a robot platform (or a set of robot platforms) or the mechanical hardware. Examples of the first category are Orocos[13], OpenRTM[14] and the Robot Operating System (ROS)[15] which is a recent attempt of standardizing middleware for mobile robotics. One slightly older example of the latter is the Japanese open source robot Pino[16]. There is also a notable activity in the creation of open source electronic design and this is summarized for example in the activities of the OpenCores[a].

The iCub[b] is one of the results of the RobotCub project, a EU-funded endeavor to create a common platform for researchers interested in embodied artificial cognitive systems[17]. Here the RobotCub project took a strong stance towards open

[a] *http://www.opencores.org*
[b] *http://www.icub.org*

source by releasing everything of the Consortium work as GPL, FDL or LGPL: this includes the mechanical and electronics design together with the software infrastructure of the iCub. The software infrastructure is based on an open source middleware called YARP which can compile cleanly on a number of operating systems (supported on Linux, Windows and MacOS) using a well-established set of tools[18].

For the design of the electronics and mechanics, we were forced to uses proprietary CAD tools, due to the absence of open source professional counterparts. This is an unfortunate situation, but there is no practical alternative at the moment. Free of charge viewers are available for all file formats employed by the project. This does not prevent however the copy or reproduction of the iCub components since 2D drawings or Gerber files suffice in manufacturing parts and printed circuit boards (PCBs).

In supporting our open source stance, considerable effort was devoted to creating an appropriate documentation of the robot. The current iCub documentation covers nearly all aspects of the robot design, from the mechanical hardware to the operating software. For RobotCub, it was decided to release all the CAD files under the GPL[c]. The associated documentation was also licensed under the GPL[d]. The YARP middleware is licensed either as GPL or LGPL.

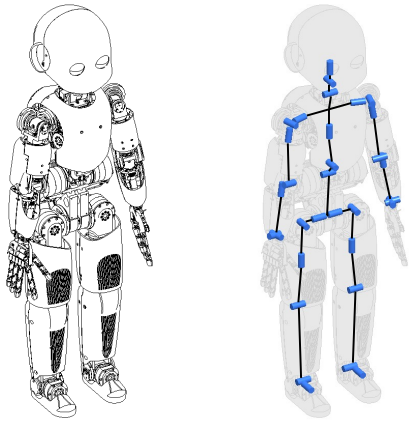

(a) (b)

Fig. 2. The iCub kinematic structure. The figure shows a CAD representation of the iCub (a) and of its kinematic structure (b). For visual clarity the representation of the eyes and hand joints has been omitted.

[c]The CAD models of the robot are available at *http://robotcub.svn.sourceforge.net/viewvc/robotcub/trunk/iCubPlatform1.1/*.
[d]The documentation of the robot can be consulted at *http://eris.liralab.it/wiki/Manual*.

3. Mechanical design of the iCub

This section describes the details of the mechanical design of the iCub robot. In its final release at the end of the RobotCub project, the iCub is approximately 1[m] tall (see Fig.1(b)), has 53 active degrees of freedom (DOF) and has a mass of approximately 24[kg].

3.1. *Design specifications*

The initial specifications for the design of the robot aimed at replicating the size of a three-year-old child[19]. In particular, it was required that the robot be capable of crawling on all fours and possess fine manipulation abilities. For a motivation of why these features are important, the interested reader is referred to Metta et al.[17]. The initial dimensions, kinematic layout and ranges of movement were drafted by considering biomechanical models and anthropometric tables [17,20]. Rigid body simulations allowed to determine which were the crucial kinematic features of the human body to be replicated in order to perform the set of desired tasks and motions[17,21]. These simulations also provided joint torques requirements: these data were then used as a baseline for the selection of the robot's actuators. The final kinematic structure of the robot is shown in Fig.2(b). The iCub kinematic structure has several peculiar features which are rarely found in humanoid robots. The waist features a three DOF torso which considerably increases the robot's mobility. Moreover the three DOF shoulder joint is constructed such that its three axes of rotation always intersect at a single point. The list of the main DOF of the iCub robot is listed in Table 1; for more detailed information the reader shall refer to the official iCub documentation[e].

3.2. *Actuators*

To match the aforementioned torque requirements several actuator technologies were considered[22,23]. Among the various alternatives rotary electric motors coupled with speed reducers were preferred because of their higher robustness and reliability. In total three modular motor groups with different characteristics were developed; this allowed their reuse throughout the main joints of the robot. All of them comprise a Kollmorgen-DanaherMotion RBE type brushless frameless motor[f] and a CSD frameless Harmonic Drive flat speed reducer[g] (see Fig. 3). Brushless motors have a very good power density and generally outperform conventional brushed DC motors. Harmonic Drive speed reducers are very light, have practically no backlash, and allow very high reduction ratios in small spaces. The use of frameless components

[e] *http://eris.liralab.it/wiki/ICubForwardKinematics*
[f] Kollmorgen DanaherMotion product website:
http://www.kollmorgen- seidel.de/website/com/eng/download/document/200512291032290.
[g] HarmonicDrive product website:
http://www.harmonicdrive.net/media/support/catalogs/pdf/csd-shd-catalog.pdf.

	degree of freedom	range of motion [deg]	
shoulder	pitch	-95	+10
	roll	0	+160
	yaw	-37	+80
elbow	flexion/extension	+5	+105
	pronation/supination	-30	+30
wrist	flexion/extension	-90	+90
	abduction/adduction	-90	+90
waist	roll	-90	-90
	pitch	-10	+90
	yaw	-60	+60
hip	flexion/extension	-120	+45
	abduction/adduction	-30	+45
	rotation	-90	+30
knee	flexion/extension	0	+130
ankle	flexion/extension	-60	+70
	abduction/adduction	-25	+25
neck	pan	-90	+90
	tilt	-80	+90
	roll	-45	+45

Table 1. The joints of the iCub. The table lists the main joints of the iCub robot and their respective range of motion.

allows further optimization of space and to avoids the unnecessary weight of the housings. The characteristics of the actuator modules are the following:

- the high power motor group: capable of delivering 40Nm of torque, it is based on the RBE 01211 motor and a CSD-17-100-2A Harmonic Drive, and has, roughly, a diameter of 60mm and a length of 50mm.
- the medium power motor group: capable of delivering 20Nm of torque, it is based on the RBE 01210 motor and a CSD-14-100-2A Harmonic Drive, and has, roughly, a diameter of 50mm and a length of 50mm.
- the low-power motor: capable of delivering up to 11 Nm it is based on the RBE 00513 motor and a CSD-14-100-2A Harmonic Drive and has, approximately a diameter of 40mm and a length of 82mm.

3.3. *Cable drives*

In the design of the robot cable drive transmissions are widely employed. Cable transmissions can be used to efficiently transmit power from an actuator to a driven link whose range of rotation is limited. Cable drives allow the transmission of power between bodies rotating along different axes with driven pulleys, stepped pulleys,

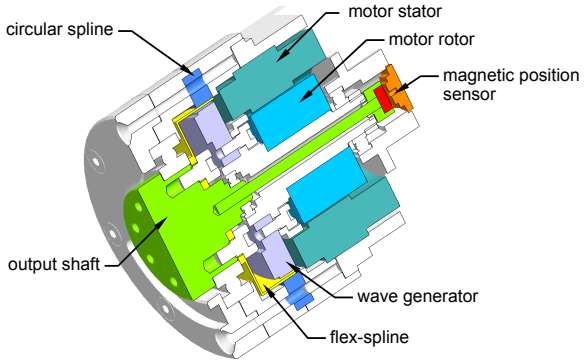

Fig. 3. Motor group cross section. The figure shows a cross section of a iCub motor group. The Harmonic-Drive and Kollmorgen brushless motor are clearly visible.

pinions, and idle pulleys. Whenever space is limited they are a good alternative to geared transmission. Despite this kind of transmission generally has a lower mechanical stiffness than gears, if designed properly, it generally allows to obtain higher efficiencies. Moreover cable drives can be used to construct epicyclic transmission mechanisms similar to the one introduced by Salisbury et. al.[24,25] and refined by Townsend[26]. In normal "serial" manipulators all the motors and speed reduction units are mounted directly on the joints, thus increasing the inertial loads on the motors. Instead by using coupled cable transmission the joints can be driven remotely: motors can thus be mounted in the proximity of the joint rather than on the joint itself. A mechanism of this kind has several advantages among which are a more compact size and lower weights and inertias if compared to standard serial designs. Another advantage is that this kind of transmission generally allows to obtain larger workspaces. However it is generally affected by some drawbacks such as higher mechanical complexity (therefore higher manufacturing costs and longer assembly time) and less intrinsic robustness. Examples of the implementation of cable drives can be found in the shoulder, elbow, torso, hip and ankle joints.

Let us consider, for illustrative purposes, the assembly of the two stage shoulder roll joint, represented in Fig.4 and Fig.5. The output shaft of the motor block comprises a pulley that is connected to an idle pulley, that is coaxial with the main motor group of the shoulder joint. This connection is obtained with two high resistance steel cables (1.5[mm] cross sectional diameter), manufactured by Carlstahl[h] and represented in pink and purple in Fig5(a). Because cables can only transmit forces through tension, two of them are always necessary to obtain forward and backward motion. Two other cables (represented in red and blue in Fig5(a)) connect the idle pulley to the output assembly with pulleys that intersect at a 90[deg]

[h]Manufacturer's website: *http://www.carlstahl.de/*.

angle, thus constituting the second stage of the transmission. Since the two cables cannot be wound on the same cylindrical surface (as suggested by Townsend[25]), a stepped pulley is employed to allow the correct cable routing.

3.4. *Materials selection*

The total weight design specification was particularly difficult: special care had to be taken in the design of structural elements to avoid adding mass. For what concerns the materials, the majority of the parts of the robot were fabricated with the Al6082 aluminum alloy. With its ultimate tensile strength (UTS) of 310[MPa] and roughly the typical density of aluminum 2700[kg/m^3], Al6082 is among the best materials in the 6000 alloy series[i]. For these reasons it was widely employed for all the parts that did not require particular resistance characteristics. Another material that has been employed id the Al7075 aerospace aluminum alloy because of its excellent strength to weight ratio. The use of zinc as the primary alloying element results in a strong material, with good fatigue strength and average machinability. The density of Al7075 has a density of 2810[kg/m^3] which is slightly higher than normal aluminum; its UTS of 524[MPa][j] is comparable with that of medium quality steels and make it one of the toughest types of aluminum alloys currently available. Components with more demanding mechanical properties were therefore manufactured with this material. Finally, highly stressed parts (such as joint shafts) were obtained from the high resistance stainless steel 39NiCrMo3. This material, known in the AISI standard as AISI9840, is a nickel-chromium-molybdenum steel, that exhibits a good combination of strength, fatigue resistance, toughness and wear resistance. Its UTS is high, around 1.2[GPa][k].

3.5. *The arm and elbow assemblies*

The iCub arm has two joints: a three DOF proximal "shoulder" joint and a rotational distal "elbow" joint (see Fig.4). The shoulder movements are obtained by means of a cable driven epicyclic transmission of the kind described in section 3.3 which is shown in Fig.5(a). The three motors driving the shoulder are housed in the upper-torso aluminum frame. The first motor actuates directly the shoulder pitch joint whereas the second and third motors actuate two pulleys that are coaxial with the first motor. These pulleys have slightly different primitive diameters thus producing a transmission reduction equal to the ratio of their diameters. The pulley motion is then transmitted to the shoulder roll and yaw joints through a second set of idle pulleys (see Fig.5(a) and Fig.5(b)). As a result the shoulder joint has its

[i] Al6082 Matweb datasheet:
http://www.matweb.com/search/datasheet_print.aspx?matguid=fad29be6e64d4e95a241690f1f6e1eb7.
[j] Al7075 Matweb datasheet:
http://www.matweb.com/search/datasheet_print.aspx?matguid=9852e9cdc3d4466ea9f111f3f0025c7d.
[k] 39NiCrMo3 Matweb datasheet:
http://www.matweb.com/search/datasheet_print.aspx?matguid=697130f21da64542a68bf61911f2f495.

three axes of rotation intersecting at a single point (which is a typical characteristic of robotic wrist mechanisms) thus allowing "quasi"-spherical movements.

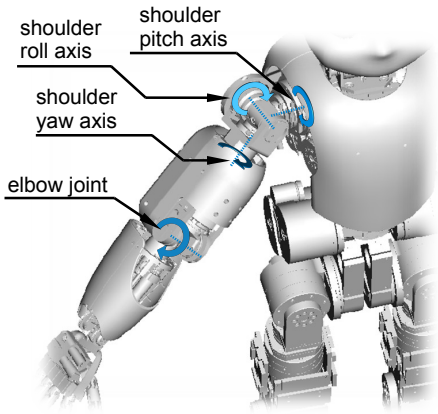

Fig. 4. The iCub arm. The figure represents a CAD view of the arm of the iCub and its three DOF shoulder joint and one DOF elbow joint.

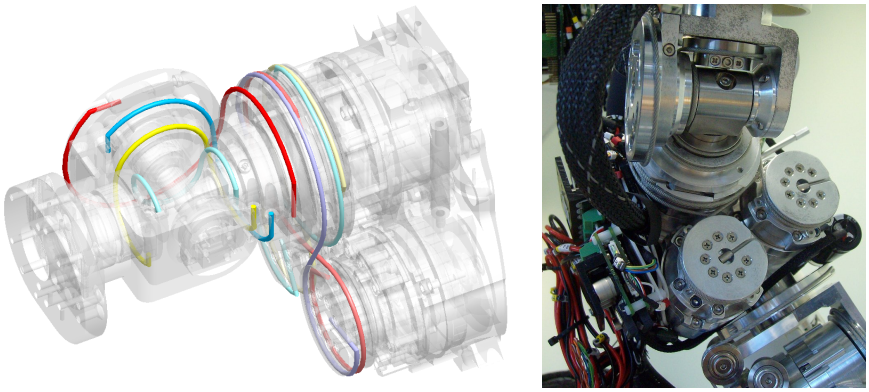

(a) (b)

Fig. 5. The shoulder joint. The figure shows a CAD view of the shoulder joint mechanism with a highlight of the cable transmission system (a). The figure also shows a photo of a bottom view of the shoulder joint (b).

This unconventional construction introduces kinematic couplings between the different motions. Because of this coupling however the relation between the displacements and the torques at motor and joint level is not straightforward. The technique outlined by Tsai for robotic wrist mechanisms[27] is particularly convenient for the analysis of complex epicyclic transmissions and allows to derive these

relations for the iCub shoulder mechanism[28].

The one DOF elbow joint is rather simple in its design. The output link is driven through a pulley system which transmits the power from the motor group. The motor is housed at the center of the assembly oriented 90[deg] with respect to the axis of rotation of the elbow. A six-axis force-torque sensor is mounted at the interface between the shoulder and elbow assembly.

3.6. *The forearm and hand groups*

The hand of the iCub has been designed to enable dexterous manipulation as this capability is crucial for natural grasping behaviours (which are in turn fundamental for our research in cognitive systems). The hand of the iCub has 19 joints but is driven by only 9 motors: this implies that group of joints are under-actuated and their movement is obtained with mechanical couplings. Similarly to the human body most of the hand actuation is in the forearm subsection. In particular, seven out of the nine motors driving the hand joints are placed in the forearm assembly. Given the limited amount of space available 0.36 to 2.57[W] brushed DC electric motors were employed. These electric motors are coupled to multistage planetary speed reducers (whose reduction ratios vary from 159:1 to 256:1) to obtain the desired torques. The output shaft of the motors is connected to capstans which wind and unwind the steel cables that drive the phalanges movements.

The tendon arrangement is extremely critical; therefore the cable routing had to be done with extreme care and neatly organized according to specified guidelines [1] (see Fig.6(b)). Moreover each tendon has to be tensioned properly: this was achieved by inserting double screwed tensioners along each cable.

The wrist is driven by a differential transmission mechanism of the type described in section 3.3. On the other hand the flexing of the fingers is directly driven by the motors while their extension relies on a spring return mechanism, thus reducing the overall complexity of the device. The motion of the proximal phalanx and medial and distal phalanges are independent for the thumb, the index and the middle finger. The ring and small finger motions are coupled and driven by a single motor. Finally two motors, placed directly inside the hand assembly, are used for adduction/abduction movements of the thumb and of the index, ring and small fingers. The position of each phalanx is sensed by 17 small custom magnetic position sensors.

The overall size of the hand is extremely compact with its 50[mm] in length, 60[mm] in width and 25[mm] in thickness, making it one of the smallest and most dexterous of its kind. The design of the iCub hand has been addressed in greater detail in a recent paper by Schmitz et al.[29] to which the reader shall refer for additional informations.

[1]The documentation can be consulted at
http://robotcub.svn.sf.net/viewvc/robotcub/trunk/iCubPlatform/doc/assembly/tendonsHand2007.pdf.

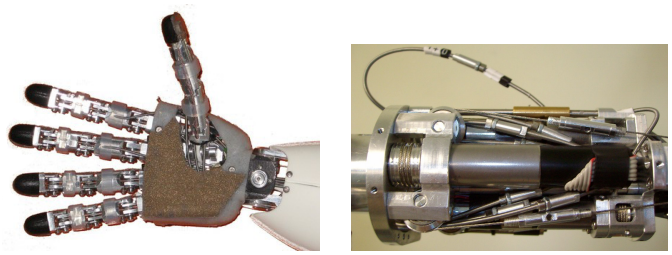

(a) (b)

Fig. 6. The right forearm and hand of the iCub. The figure shows a photo of the right hand of the iCub (a) and of the right forearm (b). The motor-capstan arrangement and the cable tensioning devices, described in the main text can clearly be seen in (b).

3.7. *The lower body and the torso*

The preliminary phases of the design process described in section 3.1 suggested that for effective crawling a two DOF waist/torso mechanism is adequate. However, a three DOF waist was preferred to increase the range and flexibility of motions of the upper body. As a result the robot can lean, sideways, forwards and backwards, and rotate its body along its sagittal axis.

The torso mechanism is also based on the differential epicyclic transmission described in section 3.3. In this case however the two base motors drive a third motor group, whose axis is orthogonal to the previous motors. The first two motors actuate jointly the pitch and roll axes whereas the third motor drives the yaw joint. The torso subassembly is shown in Fig.7.

Fig. 7. The torso of the iCub. The figure shows a photo of the 3DOF torso mechanism and in particular the construction of the differential cable drive transmission.

Since for the legs space and size constraints were not particularly critical the lower body was designed with a more standard "serial" configuration. The legs of

the iCub comprise a three DOF joint at the hip. In this joint the first DOF is driven remotely by means of a cable drive actuated by a motor which is located in the lower torso assembly (see Fig.8(a)). The leg includes a one DOF knee joint, actuated by the knee flexion/extension motor, and a two DOF ankle (see Fig.8(b)). Each ankle is actuated by a frameless brushless motor housed in the lower leg segments which drives the flexion/extension movement and by a smaller motor group for the abduction/adduction movement which is placed directly on the foot.

(a) (b)

Fig. 8. Details of the legs. The figure shows detail photographs of the legs of the iCub robot. The fisrt two axes of the 3DOF hip are shown in (a). The 2DOF ankle is shown in (b).

3.8. *The head*

The primary function of the head assembly is to move cameras in order to quickly observe the environment. Two small video cameras are therefore available on the iCub eyes (contained entirely inside the eyeballs). These cameras are moved by a three DOF eyes mechanism which allows both tracking and vergence behaviors. The compact neck mechanism has three additional DOF arranged in a serial pitch, roll and yaw configuration (see Fig.1(c)). The three neck joints are driven by brushed DC motors coupled with low backlash Gysin speed reducers, to avoid problems when performing visual tasks. The eyes movements are also achieved with three DC brushed motors which drive the eyes with toothed belts (see Fig. 9). The belts can be tensioned by means of apposite tensioning guides which are included in the mechanism. Besides the video camera and the video processing boards the head also contains the following elements:

- an XSense MTx inertial sensor, which measures the three components of linear accelerations and of angular velocities;
- a PC104 which is used for high level motor control (see section 4.1);
- two small omnidirectional microphones, for auditory input;
- a MCP and two MC4 boards (see section 4.2) which are used to control the neck and eyes motors;

- facial expression boards, which control a set of LED's that represent the facial expressions.

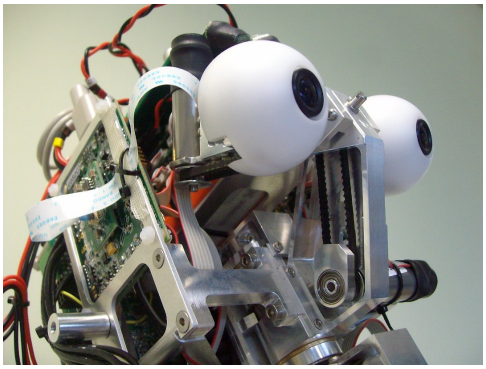

Fig. 9. Eyes mechanism. The figure shows a photo of the eyes mechanism; in particular the toothed belt transmissions of the eyes tilt and pan axes can be seen.

4. Electronics and sensors

4.1. *PC104*

The PC104 card is used in general for the bidirectional communication of iCub with the external control station. It is based on a Intel Core 2Duo 2.16[Mhz] Pentium processor and has 1GB of RAM, and the sensors acquisition and control electronics. The data to and from the different robot parts are transferred over several CAN bus lines. As the gradual improvements and addition of sensors (see following sections) required an increase of data throughput in its latest revision the board interfaces with ten CAN bus ports.

4.2. *Motor Control boards*

The arms' brushless motors are controlled with the BLL (BrushLess Logic) and the BLP (BrushLess Power) electronic boards shown in Fig.10(a). The BLL board processes the various signals provided by the sensors and generates the control signals that govern the motion of the motors. These signals are then passed to the BLP board which contains the actuator power drivers: the voltages applied to the three phases are controlled by the amplifiers with pulse width modulation (PWM). BLP boards can provide power up to 20[A] at 48[V]. Similar but smaller boards have been developed to drive small, low power DC motors. The power board and the controller board (which drives four motors independently) are conventionally called MCP and MC4 respectively. A MCP and three MC4 boards (see Fig.10(b)) can be used to control up to 12 DC motors, delivering up to 1[A] at 12[V] to each

motor. The electronics are placed on-board near the motor joint assemblies. Data to and form BLL and MC4 boards are exchanged through CAN bus interfaces.

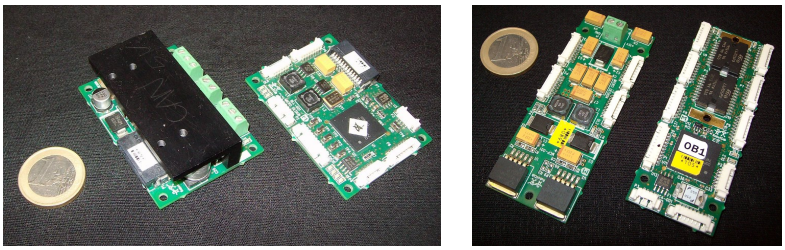

(a) (b)

Fig. 10. Motor control boards. The figure shows the custom motor control boards developed for the RobotCub project. The BLP and BLL boards for high power motor groups are shown in (a). The low power MCP and MC4 boards are shown in(b).

4.3. *Joint position sensors*

For what concerns position sensing, each actuator unit contains three Hall effect sensors integrated in the motor stator that can be used as an incremental rotary position sensor. This provides a low resolution 48*cpr* (counts per revolution) rotor position measurement which can be used for trapezoidal phase commutation. Moreover every joint angular position is sensed with an absolute 12bit angular encoder (employing the AS5045 microchip from Austria Microsystems).

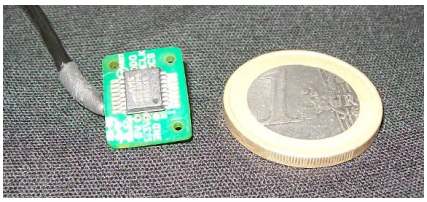

Fig. 11. AEA board. The figure shows a photograph of the 12 bit AEA encoder board.

In most cases there is no room to fit a position sensor in the frontal part of the motor groups since all parts move with respect to the frame. For this reason it was necessary to locate the position sensor in the rear of the motor. To do this the movement of the output link is transmitted through the motor's rotor hollow shaft with a thin shaft that carries the magnet for the sensor: this particular arrangement can be seen in Fig.3.

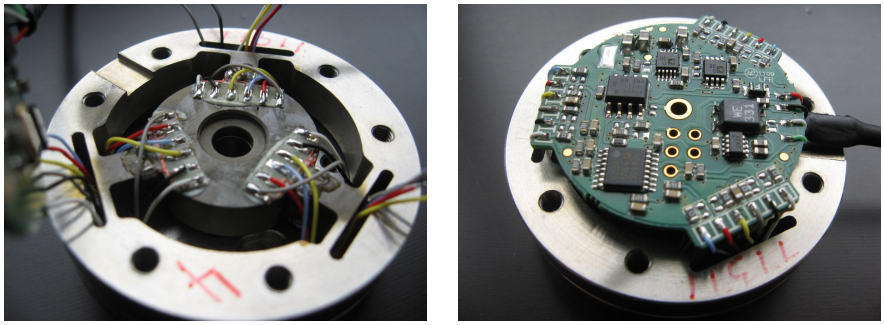

(a) (b)

Fig. 12. Six-axis force-torque sensor. The figure shows photos of the sensors' three-spoke structure (a), and the integrated electronic board (b).

4.4. *Six-axis force-torque sensor*

The iCub arm also comprises a six-axis force-torque sensor [21]. The sensor load cell is based on a three spoke structure machined from stainless steel Fig.12(a). On each side of each spoke a semi-conductor strain-gage is mounted: opposite strain gages are connected in a half Wheatstone's' bridge configuration. The sensor integrates an electronic board for the data acquisition and signal conditioning Fig.12(b). The board samples six analog channels with an INA118 instrumentation amplifier: each input is connected to one of the six aforementioned half Wheatstone's' bridges. The analog to digital conversion is performed by an AD7685 converter on the multiplexed signals of the six channels. It is besides possible to add an offset by means of a DAC. The board also allows the installation of thermal compensation resistors that minimize the thermal drift effects of the semi-conductor strain gages. All the operations are managed with a 16bit DSP from Microchip (dsPIC30F4013) which also provides digital signal filtering and the linear transformation needed to project the signals of the strain gages to the force/torque space. The data are finally broadcast through a CAN bus interface at a frequency of 1[kHz].

4.5. *Pressure sensors for tactile feedback*

Humanoid robots are required to sustain increasingly complex forms of interaction (e.g. whole hand or whole arm grasping and manipulation[30], etc.). In these cases the location and the characteristics of the contact cannot be exhaustively predicted or modeled in advance. Skin-like sensors and sensing methods are therefore required for processing distributed tactile information. The problem is not new and some pressure sensing technologies for humanoid robots were studied recently[31,32].

We have equipped the hands of iCub with a distributed pressure sensing system based on capacitive technology[33,34]. This technology is based on modules which yield 12 independent measurements from 12 corresponding pressure sensing ele-

ments, called taxels in the following. The basis of each taxel is constituted by a round metal pad which is obtained on a flexible PCB. Flexible PCBs can be bent to cover generic curved surfaces and the shape can be engineered to optimize covering or curvature of the robot surface. The flexible PCBs are then covered with a thin layer of soft silicone foam, which is roughly 2.5[mm] thick. This silicone layer acts as the dielectric medium of a capacitor. The foam is covered by an outer layer, which can be obtained either from conductive Lycra or from conductive silicone. This layer is connected to ground and enables the sensor to respond to objects irrespective of their electrical properties (unlike consumer electronics products based on the same technology). In addition, this layer reduces electric noise from the environment. When pressure is applied to the sensor, this conductive layer gets closer to the round pads on the PCB thereby changing their capacitance. We use this change in capacitance as an estimation of the pressure applied to the sensor surface. The taxels are connected to a capacitive to digital converter chip (AD7147 from Analog Devices), which sends the measurements over an I^2C serial bus. The data of up to sixteen modules (for a total of 192 taxels) are collected by a small micro-controller board, which can then relay them to the main CPU via CAN bus.

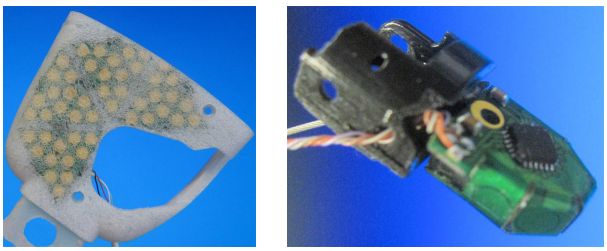

(a) (b)

Fig. 13. Tactile pressure sensors. The figure shows a photograph of the iCub palm with embedded capacitive pressure sensors (a), and a detail of the pressure sensing fingertip (b).

In the first version of iCub these pressure sensors have been embedded in the palm, the fingertips and the forearm (as shown in Fig.16(a)), to enhance the manipulation capabilities of the robot. In particular, the skin of the palm incorporates four triangular modules (see Fig.13(a)), each of the five fingertips comprises one module (see Fig.13(b)), and the forearm covers contain 23 modules. This arrangement results in a total of 384 independent sensitive elements per arm.

4.6. *Communication bus*

Control cards, skin sensors and force-torque sensors communicate on several 1Mbit/s CAN bus ports. The network is characterized by a star-like topology, with all branches converging on the PC104 CPU. Ten CAN sub-networks (roughly one for each body segment, and two dedicated for skin sensors) join at a central node which

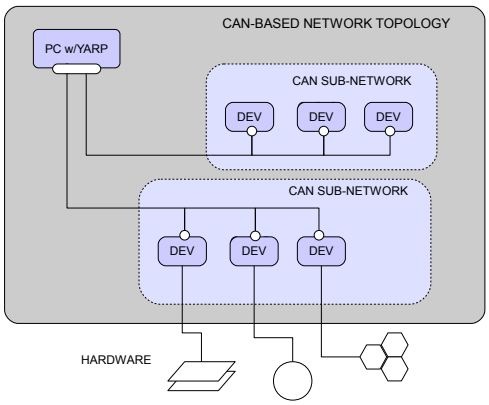

Fig. 14. iCub bus diagram. The figure shows a diagram of the current communication bus arrangement of the iCub. The control boards are called DEV int the figure.

is constituted by the PC104 described in section 4.1. This network architecture is represented in Fig.14.

5. iCub2

The first version of the iCub robot was developed and constructed four years ago. Since then it has intensively been used by several partners and institutions[m]: this allowed to reveal several critical aspects in its initial design. We therefore began the development of a new version of the iCub (tentatively called iCub2) which is now almost complete. The most relevant improvements are described in the following sub-sections.

5.1. *Joint torque sensing*

The requirement for the robot to interact safely and robustly with humans and its surrounding environment is particularly difficult to fulfill. To achieve this joint torque feedback is essential. We therefore developed torque sensors for the main joints of the iCub. All the sensors are based on the piezo-resistive effect of semiconductor strain gages (SSG). When loads are applied the sensing elements and the SSG which are attached to them deform. This deformation is accompanied by a change in resistance which is proportional to the applied torque. The signal conditioning is preformed by microcontroller boards similar to the one described in section 4.4. The sensors allow the measurement of joint torques with 16 bits of resolution at a frequency of 1[kHz]. As the constraint was to maintain all the functional dimensions of the iCub unchanged, the development of the sensor for the

[m]A comprehensive and up to date list can be found in the website *http://www.icub.org*

shoulder joint (which are shown in Fig.15(a)) was particularly complicated[35]. For the lower body instead it was possible to develop a sensor with radial, controlled deformation, spoke features, that can seamlessly be integrated in the motor groups (see Fig.15(b)). Finite element structural simulations were employed to optimize the final sensor geometries. Although the current loop frequency is limited by the CAN bus network throughput, in the near future it will be possible to close torque feedback loops at 3[kHz] by relying on a new control card design (see section 5.6). The

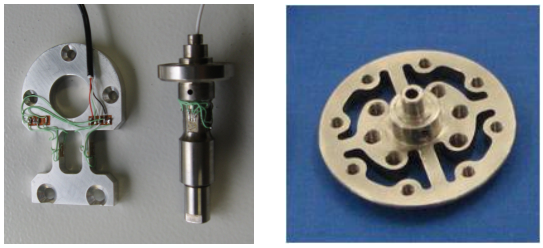

(a) (b)

Fig. 15. Joint torque sensing. The figure shows a photograph of the iCub shoulder joint torque sensors (a), and the "modular" joint torque sensor developed for the lower body (b).

addition of joint torque sensing also required significant upgrades to the firmware and software currently used to control the robot[36].

5.2. *Extensive tactile feedback*

Besides joint torque sensing the sense of touch is among the principal sensing modalities required to work closely and interact safely with humans and more in general with the environment. Touch can provide a reliable source of information to guide exploratory behaviors as required for example in machine learning. For this reason the exterior surfaces of iCub2 have been extensively covered with the pressure sensitive elements described in section 4.5. As shown in Fig.16 the "skin" tactile sensors will be embedded in the fingertips, the palms, the forearms, the upper arm segments, the torso, the upper leg segments, the knees, the lower leg segments and the feet, for a total of approximately 4200 taxels. This, to our knowledge, makes iCub2 the humanoid robot with the highest number of pressure sensitive points. The processing of the vast amount of data streaming from these sensors will be an interesting technological challenge which is currently being addressed in the context of the RoboSKIN[n] FP7 European project.

[n]http://www.roboskin.eu/

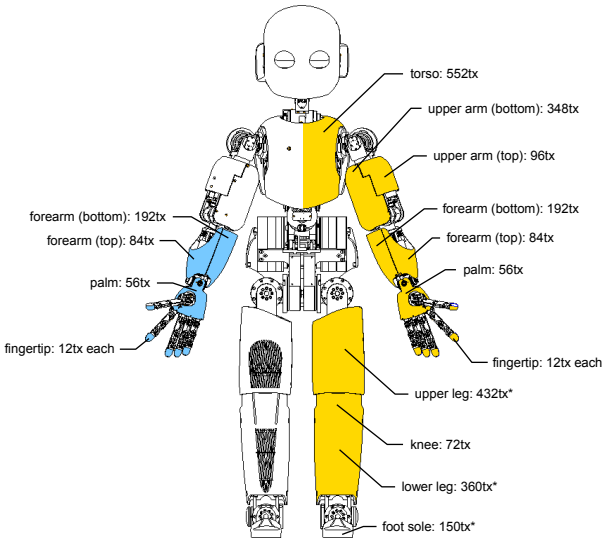

Fig. 16. Pressure sensing surfaces of the iCub. The figure shows the covers of the iCub covers with embedded pressure sensors. The surfaces colored in blue (a) show the pressure sensing elements of the first version of iCub. The surfaces colored in yellow (b) show the skin coverage of iCub2. The figure also indicates the number of taxels for each body segment. The numbers with the asterisk are to be intended as approximate as the design of those surfaces is currently being finalized.

5.3. *Head and eyes redesign*

It was noticed that in particular operating conditions the neck motor would overheat quickly, thus indicating that they were probably under-dimensioned. A first revision of the neck mechanism, still based on the serial joint configuration, was proposed by Rodriguez[37]. The proposed solution was based on the use of Harmonic Drive speed reducers and four-bar linkages as key elements of the transmission. However the design was not entirely compatible with size and space constraints, and was therefore modified. This variant is based on a "parallel" actuation scheme with cable drives. The new solution is partly inspired by the design of the robot COG by Brooks et al.[38] which has also been employed in the construction of the MERTZ robot head [39]. As described in section 3.3, epicyclic transmissions are a very effective way to reduce the driven masses and inertias. In the final design the new head assembly weights approximately 1.05[kg] less than the first version of the head. With its 8[Nm] peak torque on the pitch and roll axes, the new neck mechanism also allows a three-folds increase of the delivered output torque.

The eyes mechanism has also been revised. The original design was found to be critical in two senses:

- rapid eye movements were obtained with brushed DC motors which em-

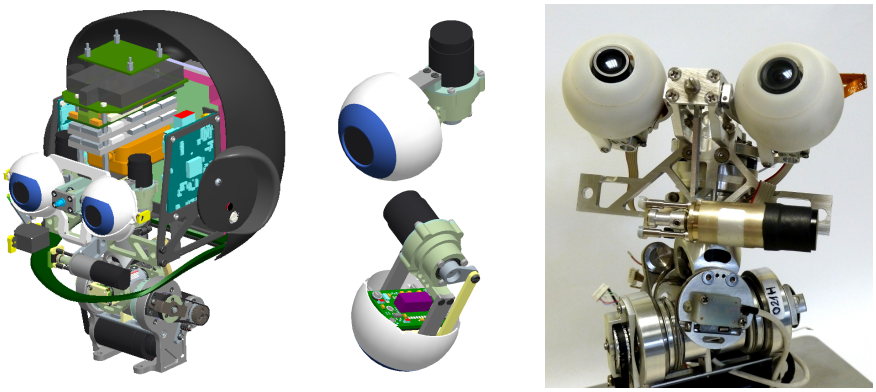

(a) (b) (c)

Fig. 17. Design revision of the iCub head. The figure shows two CAD views of the new version of the iCub head and eyes (a) and (b), and a photo of the head without the electronics (c).

ployed low reduction ratio planetary speed reducers. This introduced significant backlashes in the transmission, thus complicating the control, and in general the achievement of visual tasks.

- the tensioning of the toothed belt transmission had to be performed manually. This was problematic in terms of accuracy of the camera positioning.

The first issue is commonly solved by employing zero-backlash Harmonic Drive speed reducers, as done also by Asfour et al.[40] in the tilt joint of the ARMAR-III humanoid head. Rodriguez suggested this solution[37] as well; moreover he proposed to solve the second issue by replacing the transmission belts with low play, rigid four bar linkages. Since the elegant solution proposed by Rodriguez[37] introduced a mechanical coupling between the eyes pan and tilting motions we preferred to maintain the current eyes mechanism configuration while improving the precision by the addition of Harmonic Drive gears. A CAD view of the new iCub head is shown in Fig.17. The new neck design also features a two piece eyeball whose outer part can easily be removed to fine-tune the positioning of the cameras.

5.4. *Optical encoders*

Currently the configuration of the robot is measured by means of the magnetic joint positions sensors described in section 4.3. Brushless motors are instead driven with a "standard" trapezoidal PWM profile strategy based on the feedback of three digital Hall effect sensors placed in the motor stator. These sensors provide a low resolution 48*cpr* (counts per revolution) signal which causes slight vibrations when driving the motor at low speeds. To solve this issue and to implement more advanced field oriented control (FOC) strategies we developed and tested an extremely compact custom optical encoder with 8192*cpr* resolution. We successfully completed the

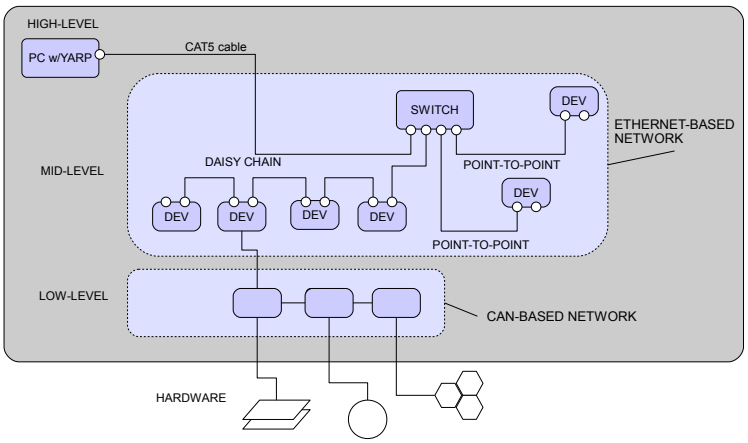

Fig. 18. Ethernet bus diagram. The figure shows a diagram of new Ethernet based network architecture.

preliminary testing and are now integrating this subsystem in all the major joints of the robot.

5.5. *Control boards revision*

The control boards were improved in several ways. More in detail the first release of the BLL boards, described in section 4.2, had several issues for what concerned the phases current measurement system. This system has been improved and is now capable of providing a reliable, high bandwidth, 13bit current measurement. Moreover as new sensors were added to the robot (e.g. see section 5.4) the board I/O ports had to be revised, without however substantial changes. Finally the boards firmware has been thoroughly optimized with respect to its first stable release.

5.6. *Ethernet bus*

Besides the aforementioned upgrades the whole sensory motor architecture is being deeply revised. Since the current network (based CAN buses) limits the data throughput, a new Ethernet based network has been developed. The new architecture will be configured hierarchically with "mid-level" control boards called DEV in the following, supervising the operation of "low-level" boards (as represented in Fig18). The higher layer of the architecture will communicate on an Ethernet bus, whereas the lower level boards will employ an efficient and robust CAN transmission protocol. The solution which we are currently investigating is based on a flexible Ethernet design, where the DEVs, present two plugs for connection with a CAT5 cable. The DEVs can thus be connected either in daisy chain or in point-to-point or even in a mixture of them.

6. Conclusions

The first part of this article presented the development of the iCub robot, which is currently being used in several robotics laboratories worldwide for research in embodied cognition[o]. In the second part the most relevant upgrades which are being integrated in the second version of the robot (namely iCub2) have been described. The robot features a combination of various technologies which make it unique; among these full joint torque feedback, extensive pressure sensing, open hardware and software can be cited as the most important. We hope that these features will make iCub2 the platform of choice for the emerging fields of artificial intelligence, motor control and developmental cognition.

Acknowledgments

This work has been supported by the European Commision RobotCub IST-FP6-004370, CHRIS IST-FP7-215805 and RoboSKIN ICT-FP7-231500 projects.

We would like to thank and to acknowledge the contributions to this project of Mattia Salvi, Diego Torazza, Fabrizio Larosa, Marco Accame, Claudio Lorini, Bruno Bonino, Andrea Menini, Davide Gandini, Emiliano Barbieri, Roberto Puddu, Charlie Sanguineti, Marco Pinaffo and all the people who have contributed to the construction, maintenance and design of the iCub, whose help has been essential to the completion of this work.

References

1. Masato Hirose and Kenichi Ogawa. Honda humanoid robots development. *Philosophical Transactions of the Royal Society*, 365(1850):11–19, 2007.
2. I.W. Park, J.Y. Kim, J. Lee, and J.H. Oh. Mechanical design of the humanoid robot platform HUBO. *Advanced Robotics*, 21(11):1305–1322, 2007.
3. Tatsuzo Ishida, Yoshihiro Kuroki, and Jinichi Yamaguchi. Mechanical system of a small biped entertainment robot. In *Proc. IEEE/RSJ Int. Conf. on Intelligent Robots and Systems (IROS)*, pages 1129–1134, October 2003.
4. D. Gouaillier, V. Hugel, P. Blazevic, C. Kilner, J. Monceaux, P. Lafourcade, B. Marnier, J. Serre, and B. Maisonnier. Mechatronic design of NAO humanoid. In *Proc. IEEE Int. Conf. on Robotics and Automation (ICRA)*, pages 2124–2129, 2009.
5. K. Kaneko, F. Kanehiro, M. Morisawa, K. Miura, S. Nakaoka, and S. Kajita. Cybernetic human HRP-4C. In *Proc. IEEE/RAS Int. Conf. on Humanoid Robots (HUMANOIDS)*, pages 7–14, 7-10 2009.
6. T. Asfour, K. Regenstein, P. Azad, J. Schroder, A. Bierbaum, N. Vahrenkamp, and R. Dillmann. ARMAR-III: An integrated humanoid platform for sensory-motor control. In *IEEE/RAS Int. Conf. on Humanoid Robots (HUMANOIDS)*, pages 169–175, 2006.
7. C. Ott, O. Eiberger, W. Friedl, B. Bauml, U. Hillenbrand, C. Borst, A. Albu-Schaffer, B. Brunner, H. Hirschmuller, S. Kielhofer, et al. A humanoid two-arm system for dex-

[o]For an up to date list of the demonstrations of the robot please consult the website: *http://www.youtube.com/user/robotcub.*

terous manipulation. In *IEEE/RAS Int. Conf. on Humanoid Robots (HUMANOIDS)*, pages 276–283, 2006.
8. Kenji Kaneko, Kensuke Harada, Fumio Kanehiro, Gou Miyamori, and Kazuhiko Akachi. Humanoid robot HRP-3. In *Proc. IEEE/RSJ Int. Conf. on Intelligent Robots and Systems (IROS)*, pages 2471–2478, 2008.
9. Christopher G. Atkeson, Joshua G. Hale, Frank Pollick, Marcia Riley, Shinya Kotosaka, Stefan Schaal, Tomohiro Shibata, Gaurav Tevatia, Ales Ude, Sethu Vijayakumar, and Mitsuo Kawato. Using humanoid robots to study human behavior. *IEEE Intelligent Systems*, 15(4):46–56, 2000.
10. Akihiko Nagakubo, Yasuo Kuniyoshi, and Gordon Cheng. The ETL-humanoid system - a high-performance full-body humanoid system for versatile real-world interaction. *Advanced robotics*, 17(2):149–164, 2003.
11. T. Minato, Y. Yoshikawa, T. Noda, S. Ikemoto, H. Ishiguro, and M. Asada. CB^2: A child robot with biomimetic body for cognitive developmental robotics. In *IEEE/RAS Int. Conf. on Humanoid Robots (HUMANOIDS)*, 2007.
12. G. Cheng, Hyon Sang-Ho, A. Ude, J. Morimoto, J.G. Hale, J. Hart, J. Nakanishi, D. Bentivegna, J. Hodgins, C. Atkeson, M. Mistry, S. Schaal, and M. Kawato. CB: Exploring neuroscience with a humanoid research platform. *Advanced robotics*, 21(10):1097–1114, 2007.
13. Herman Bruyninckx, Peter Soetens, and Bob Koninckx. The real-time motion control core of the Orocos project. In *Proc. IEEE Int. Conf. on Robotics and Automation (ICRA)*, pages 2766–2771, 2003.
14. —. OpenRTM. http://www.openrtm.org/.
15. Morgan Quigley, Brian Gerkey, Ken Conley, Josh Faust, Tully Foote, Jeremy Leibs, Eric Berger, Rob Wheeler, and Andrew Y. Ng. ROS: an open-source robot operating system. In *Open-Source Software workshop at the Int. Conf. on Robotics and Automation (ICRA)*, 2009.
16. F. Yamasaki, T. Matsui, T. Miyashita, and H. Kitano. Pino the humanoid: a basic architecture. *RoboCup 2000: Robot Soccer World Cup IV*, pages 269–278, 2001.
17. Giorgio Metta, Giulio Sandini, David Vernon, Darwin Caldwell, Nikolaos Tsagarakis, Ricardo Beira, Jose Santos Victor, Auke Ijspeert, Ludovic Righetti, Giovanni Cappiello, Giovanni Stellin, and Francesco Becchi. The robotcub project: an open framework for research in embodied cognition. In *Proc. IEEE/RAS Int. Conf. on Humanoid Robots (HUMANOIDS)*, pages 13–32, 2004.
18. P. Fitzpatrick, G. Metta, and L. Natale. Towards long-lived robot genes. *Robotics and Autonomous Systems*, 56:29–45, 2008.
19. Giorgio Metta, David Vernon, and Giulio Sandini. Deliverable 8.1. Initial specification of the iCub open system, 2004. http://www.robotcub.org/index.php/robotcub/content/download/614/2215/file/D8.1.pdf.
20. Alvin R. Tilley. *The measure of man & woman: human factors in design.* Wiley Interscience, 2002.
21. Tsagarakis, N.G., Metta, G., Sandini, G., Vernon, D., Beira, R., Becchi, F., Righetti, L., Santos-Victor, J., Ijspeert, A.J., Carrozza, M.C., Caldwell, and D.G. iCub: the design and realization of an open humanoid platform for cognitive and neuroscience research. *Advanced Robotics*, 21(10):1151–1175, 2007.
22. John M. Hollerbach, Ian W. Hunter, and John Ballantyne. *A comparative analysis of actuator technologies for robotics*, pages 299–342. MIT Press, Cambridge, MA, USA, 1992.
23. Paolo Dario. Deliverable 7.2. Analysis and pre-selection of the sensor and actuator

technologies., 2004. http://www.robotcub.com/index.php/robotcub/private/deliverables/deliverable_7_2_pdf.
24. J. Kenneth Salisbury, William T. Townsend, David M. DiPietro, and Brian S. Eberman. Compact cable transmission with cable differential. Patent, Feb 1991. US 4 903 536.
25. William T. Townsend. *The effect of transmission design on force-controlled manipulator performance*. PhD thesis, Massachusetts Institue of Technology, 1988.
26. William T. Townsend and J. Kenneth Salisury. Mechanical design for whole-arm manipulation. In Paolo Dario, Giulio Sandini, and Patrick Aebischer, editors, *Robots and biological systems: towards a new bionics?*, pages 153–164. Springer, 1993.
27. Lung-Wen Tsai. *Robot analysis*. Wiley interscience, 1999.
28. Alberto Parmiggiani. *Torque control: a study on the iCub humanoid robot*. PhD thesis, Univversitá degli Studi di Genova, 2010.
29. A. Schmitz, U. Pattacini, F. Nori, L. Natale, G. Metta, and G. Sandini. In *IEEE/RAS Int. Conf. on Humanoid Robots (HUMANOIDS)*, pages 186–191, 2010.
30. Y. Ohmura and Y. Kuniyoshi. Humanoid robot which can lift a 30kg box by whole body contact and tactile feedback. In *Proc. IEEE/RSJ Int. Conf. on Intelligent Robots and Systems (IROS)*, 2007.
31. O. Kerpa, K. Weiss, and H. Worn. Development of a flexible tactile sensor system for a humanoid robot. In *Proc. IEEE/RSJ Int. Conf. on Intelligent Robots and Systems (IROS)*, volume 1, 2003.
32. Y. Ohmura, Y. Kuniyoshi, and A. Nagakubo. Conformable and scalable tactile sensor skin for curved surfaces. In *Proc. IEEE Int. Conf. on Robotics and Automation (ICRA)*, pages 1348–1353, 2006.
33. G. Cannata, M. Maggiali, G. Metta, and G. Sandini. An embedded artificial skin for humanoid robots. In *IEEE Int. Conf. on Multisensor Fusion and Integration for Intelligent Systems*, pages 434–438, 2008.
34. A. Schmitz, M. Maggiali, M. Randazzo, L. Natale, and G. Metta. A arototype fingertip with high spatial resolution pressure sensing for the robot iCub. In *IEEE/RAS Int. Conf. on Humanoid Robots (HUMANOIDS)*, pages 423–428, 2008.
35. Alberto Parmiggiani, Marco Randazzo, Lorenzo Natale, Giorgio Metta, and Giulio Sandini. Joint torque sensing for the upper-body of the icub humanoid robot. In *Proc. IEEE/RAS Int. Conf. on Humanoid Robots (HUMANOIDS)*, pages 15 –20, 7-10 2009.
36. G. Metta, P. Fitzpatrick, and L. Natale. Yarp: Yet another robot platform. *International Journal on Advanced Robotics Systems*, 3(1):43–48, 2006.
37. Nestor Eduardo Nava Rodrguez. Design issue of a new iCub head sub-system. *Robotics and Computer-Integrated Manufacturing*, 26(2):119–129, 2010.
38. Rodney A. Brooks, Cinthia Breazeal, M. Marjanovic, Brian Scassellati, and Matthew Williamson. *The Cog project: Building a humanoid robot*, page 5287. Springer, New York, 1999. Lecture Notes in Artificial Intelligence 1562.
39. L. Aryananda and J. Weber. Mertz: A quest for a robust and scalable active vision humanoid head robot. In *IEEE/RAS Int. Conf. on Humanoid Robots (HUMANOIDS)*, pages 513–532, 2004.
40. T. Asfour, K. Welke, P. Azad, A. Ude, and R. Dillmann. The Karlsruhe humanoid head. In *IEEE/RAS Int. Conf. on Humanoid Robots (HUMANOIDS)*, pages 447–453, 2008.